

# Multi-Spectral MRI Analysis of Bladder Wall Segmentation Using the Level Set Approach

---

W.J. Chi<sup>a</sup>, N. Moore<sup>b</sup>, E. McVeigh<sup>c</sup>, S. Kennedy<sup>d</sup>, Sir J.M. Brady<sup>e</sup> and J.A. Schnabel<sup>a</sup>

<sup>a</sup> Institute of Biomedical Engineering, Department of Engineering Science, University of Oxford, UK

<sup>b</sup> MRI Centre, John Radcliffe Hospital, Oxford, UK

<sup>c</sup> Oxford Fertility Unit, Institute of Reproductive Sciences, Oxford Business Park North, Oxford, UK

<sup>d</sup> Nuffield Department of Obstetrics & Gynaecology, University of Oxford, UK

<sup>e</sup> Wolfson Medical Vision Laboratory, Department of Engineering Science, University of Oxford, UK

**Abstract.** In this study we investigate cases of endometriosis with bladder involvement. The aim is to segment the bladder wall and identify any abnormal change of bladder wall thickness. T1- and T2-weighted multi-spectral magnetic resonance images (MRI) are analysed for segmenting the outer and inner wall boundaries, respectively. A level set method without re-initialisation has been used, and was found to fail on the T1-weighted images. Therefore, we propose a multi-spectral MRI analysis based on intensity profiles along the zero level set contour. This method can be used as a metric for estimating the mean bladder wall thickness and for measuring global/local edge conditions, which can be potentially used as a prior for the segmentation process.

## 1 Introduction

Endometriosis is a condition defined by the presence of endometrial glandular and stromal tissue in areas outside the uterus. It occurs most frequently in the pelvic organs and peritoneum. Endometriosis can be a debilitating condition that has a profound effect on the quality of a woman's life, causing untold misery and pain over many years. It has been estimated that approximately 9% of the general population have endometriosis (estimated range 4-20%). Endometriosis can involve different abdominal and pelvic structures. Common sites are the ovaries, uterus (utero-sacral ligaments, pouch of Douglas), bowels, and bladder. Laparoscopy is currently the gold standard method to identify the disease. The safety of the removal of the lesion will depend on their site and size. Accurate pre-operative diagnosis of deep infiltrating endometriosis is essential to inform women about the specific risks of surgery, as well as to planning surgeries more effectively in hospitals.

Acquired abdominal MR images of the patients are inspected by individual radiologists. Double reading is costly and rare. Due to the huge amount of data and the subjectivity of an individual radiologist's evaluation, there is a clinical need for automated, computerised evaluation techniques to assist in the interpretation process. In this study, we have investigated specific cases of endometriosis with bladder involvement, which requires to segment the bladder wall and identify any abnormal change of bladder wall thickness. Two pairs of images of representative patients are presented, consisting of a T1- and a T2-weighted MR axial mid-slice image of the bladder. Since urine fluids inside bladder are hyperintense on T2- and hypointense on T1-weighted images, and bladder muscles are hypointense on both T1- and T2-weighted images, a natural approach is to segment the inner bladder wall boundary from T2 image and the outer wall boundary from T1 image. All pairs of images are rigidly registered using "rreg" from the Image Registration Toolkit<sup>1</sup>. We have assumed that non-rigid deformation is negligible between the image pair.

---

<sup>1</sup> <http://www.doc.ic.ac.uk/~dr/software/index.html>

## 2 Background – Level Set Segmentation

The level set method, which has been the subject of a large amount of work in recent years, is a very elegant way to handle active contours. The basic idea is to embed the contour in a higher dimensional function  $\phi(t, x, y)$ , called the level set function. By evolving the level set function, the resulting contour  $C$  is extracted from the zero level, i.e. the contour is the zero level set of the level set function, or  $C(t) = \{(x, y) | \phi(t, x, y) = 0\}$ . The level set method is non-parametric and implicit. The contours represented by the level set function may break or merge naturally during the evolution, and any topological changes are automatically handled. The evolution is a classic optimisation problem which minimises a total energy term  $E_{total}$ . Commonly  $E_{total}$  is a weighted sum of different energy terms. The external energy term  $E_{ext}$  is the driving force to move the active contour towards object boundaries and handle topological changes. The internal energy term  $E_{int}$  comprises mathematical constraints, which for example can be a curvature constraint. There is also another energy term  $E_{pri}$ , which can incorporate any prior information.

Based on the early geodesic active contours [1, 2], variational level set methods were introduced. For example, Chan and Vese [3] proposed an active contour model using a variational level set formulation incorporating region-based information; Leventon et al. [4] proposed a variational level set formulation incorporating shape-prior information. The level set method proposed by Li et al. [5] is a particular variational level set formulation that penalises the deviation of the level set function from a signed distance function. By forcing the level set function to be close to a signed distance function, this method eliminates the need for the costly re-initialisation procedure that is used in many other level set methods to maintain a stable contour evolution. It is this method that we have adopted to generate the results in this paper due to its main advantages: it is fast, as larger time steps can be taken without becoming numerically unstable; and its initialisation is very flexible and efficient. Li et al. [5] proposed three energy terms:

$$E_1(\phi) = \int_{\Omega} \frac{1}{2} (|\nabla\phi| - 1)^2 dx dy \quad E_2(\phi) = \int_{\Omega} g \delta(\phi) |\nabla\phi| dx dy \quad \text{and} \quad E_3(\phi) = \int_{\Omega} g H(-\phi) dx dy \quad (1)$$

These are the energy terms to be minimised in  $\Omega \subset \mathbb{R}^2$ . More specifically,  $E_1$  is the internal energy since it is a function of  $\phi$  only;  $E_2$  and  $E_3$  are both external energy terms, which are based on the length of the contour and the area enclosed by the contour respectively.  $\delta$  is the univariate Dirac function,  $H$  is the Heaviside function, and  $g$  is the edge indicator function for the image  $I$  defined by  $g = \left(1 + |\nabla G_{\sigma} * I|^2\right)^{-1}$ , where  $G_{\sigma}$  is the Gaussian kernel with standard deviation  $\sigma$ .

Minimisation of these energy terms with respect to  $\phi$  is solved by the Euler-Lagrange equation, which computes the first variation (or the Gâteaux derivative) of  $E_{total}$ , denoted by  $\partial E_{total} / \partial \phi$ :

$$\frac{\partial \phi}{\partial t} = - \frac{\partial E_{total}}{\partial \phi} = \alpha \left[ \Delta \phi - \text{div} \left( \frac{\nabla \phi}{|\nabla \phi|} \right) \right] + \beta \delta(\phi) \text{div} \left( g \frac{\nabla \phi}{|\nabla \phi|} \right) + \gamma g \delta(\phi) \quad (2)$$

where  $\partial\phi/\partial t$  is the gradient flow that minimises the functional  $E_{total}$ . In our implementation, if we let  $L(\phi_{i,j})$  be the approximation of the right hand side in (2) and let  $\tau$  be the time step, then the iteration scheme can be written as  $\phi_{i,j}^{k+1} = \phi_{i,j}^k + \tau L(\phi_{i,j}^k)$ .

### 3 Multi-Spectral Analysis of Level Set Intensity Profiles

Once T1 and T2 images are rigidly registered, a sequential segmentation approach is performed using the level set without re-initialisation method as presented above. As shown in Figure 1a, a level set evolution was initialised with a rectangle inside the bladder on T2-weighted image. The result shown in Figure 1b was the segmentation of inner bladder wall. This segmentation is straight forward because of the homogeneous high intensity within the bladder on the T2-weighted image. The resulting level set function is then used as the initialisation for second evolution in the T1-weighted image (Figure 1e), in order to find the outer bladder wall. However, the segmentation on the T1-weighted image can be compromised by MR bias field effect, low contrast between organs, complexity of abdominal structures, or a combination of different effects. Figure 1f shows an example when the final result underestimates the outer wall boundary due to MR bias field effect causing artificial higher intensities on the anterior side of bladder (top on Figure 1f). Figure 1c and Figure 1g show zoomed-in segments of the corresponding region of the T2- and T1-weighted image respectively.

Segmentation results from the level set method are rarely definitive, especially as the method can fail for a number of reasons and is sensitive to parameter selection. Further analysis is needed to ensure our findings and possibly to act as prior to guide the segmentation process. We propose to perform a multi-spectral analysis of the intensity profiles of the T1- and T2-weighted image along the zero level set normal directions. The first step is to compute the unit normals along the zero level set result from the T2 segmentation. On Figure 1c and Figure 1g, unit normals of the resulting T2 contour were drawn as blue arrows overlaid on both T1- and T2-weighted images. For traditional level set methods, where the level set function  $\phi$  is a signed distance function, unit normals can be found simply by computing the normalised gradient of  $\phi$ ,  $\nabla\phi/|\nabla\phi|$ . For Li's level set method without re-initialisation, i.e. when  $\phi$  is not a signed distance function, unit normals were computed from a signed distance function  $\psi$  of the resulting contour. The second step is to search for intensity values along each unit normal. Pixel intensities were extracted from both T1- and T2-weighted images, and two-dimensional arrays of these intensity profiles were constructed. Figure 1d and Figure 1h display two segments of these arrays for the T2- and T1-weighted images, respectively. The third step is to analyse these intensity profiles. For this, three types of intensity profiles are plotted. Figure 1i shows the global mean profile, obtained from averaging all intensity profiles along the contour. This clearly shows a very distinctive profile across the bladder wall, where the T2 profile appears to have a concave shape, viz. a constant intensity inside the bladder, a sharp intensity decrease at the inner wall boundary, and a sharp intensity increase at outer wall boundary, the latter of which is also matched by the T1 profile. Mean bladder wall thickness can be interpreted by the spread of the concave region, which is about 4 mm in this case. Figure 1j shows a local mean profile averaging over the zoomed-in segment in Figure 1c and Figure 1g. Here it also shows a good profile which implies a higher level of confidence in the local edges, which can be exploited for relaxing constraints to overcome local minima in order to reach the correct boundary. Figure 1k shows an individual profile at the centre of the zoomed-in segment, which demonstrates good edges but a higher sensitivity to noise; thereby, we prefer to use the mean profile over a local segment to represent local intensity profiles.

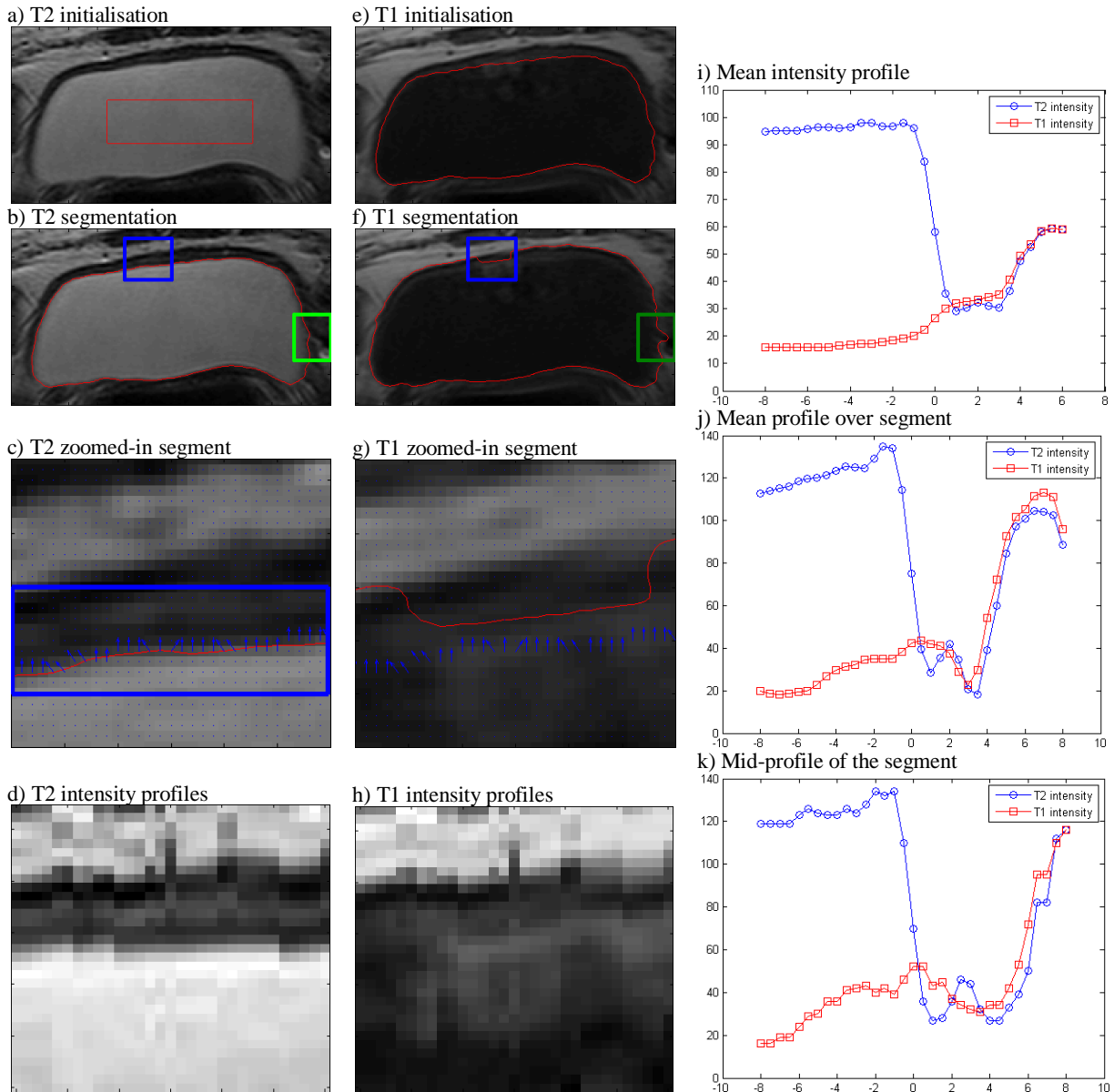


**Figure 1** Analysis of patient 1 data. (a) Initialising T2 segmentation with a rectangle. (b) Resulting contour on T2 image. Two local segments will be analysed (blue and green rectangles). (c) Zoom-in of the blue segment with unit normals overlaid (highlighted blue rectangle). (d) Array of T2 intensity profiles extracted along the normals. (e) Initialising T1 segmentation using the T2 zero level set. (f) Resulting contour on T1 image. (g) Zoom-in of the blue segment on T1 image, showing outer wall boundary underestimated. (h) Array of the corresponding T1 intensity profiles. (i) T1 and T2 mean intensity profiles. The x-axis is distance away from the contour in mm. The y-axis is image intensity. (j) T1 and T2 mean intensity profiles over the blue segment. (k) The mid-profile (one single profile) of the blue segment.

## 4 Discussion and Conclusion

Good profiles as those in Figure 1 are not always present. Even on the same set of images, weak local profiles may exist. Figure 2 shows another zoomed-in region of the previous image pair. Figure 2b illustrates that the segmentation of the T1-weighted image can overestimate the outer wall boundary, which may be due to noise. This scenario is reflected in a less strong local intensity profile plotted in Figure 2c. Again, this information can act as a prior for the segmentation process, which would enhance the edge constraint to trap the evolution at the local minimum. For the measurement of bladder wall thickness, this local profile also indicates a thinner bladder wall at this location as the spread of the concave region decreases from the mean. In an extreme case of a very weak edge shown in Figure 3, the concave region in a local mean profile was found to be of a completely flat

appearance. Choosing a higher weight for the edge constraint will not have much effect since there is no observable intensity gradient. Nevertheless, in this case we can still estimate the mean bladder wall thickness from the global mean intensity profile.

In our current investigations, we are incorporating the local intensity priors into a coupled level set framework, for a more robust and accurate bladder wall segmentation using multi-spectral MRI.

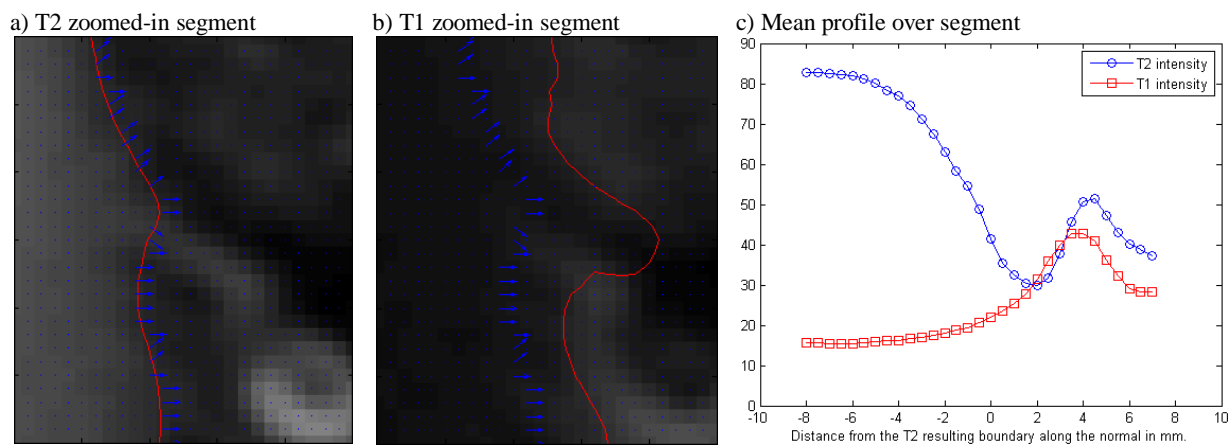


**Figure 2** Analysis of local green segment in **Figure 1**. (a) Zoomed-in region on T2 image, where boundary is overestimated. (b) Zoomed-in region on T1 image. (c) Mean T1 and T2 intensity profiles averaging over the segment in (a) and (b).

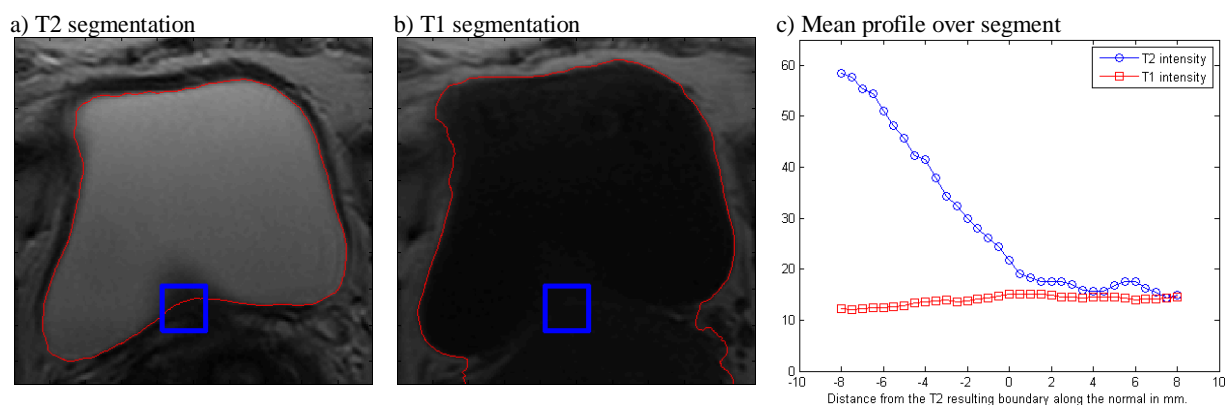


**Figure 3** Analysis of patient 2 data. (a) Resulting segmentation on T2 image. (b) Sequential segmentation on T1 image with weak boundaries. (c) Mean T1 and T2 intensity profiles averaging over the local segment in blue rectangle in (a) and (b).

## Acknowledgement

This project is funded by the Oxford Biomedical Research Centre (OxBRC), National Institute for Health Research (NIHR).

## References

1. Caselles, V., R. Kimmel, and G. Sapiro, *Geodesic active contours*. International Journal of Computer Vision, 1997. **22**(1): p. 61-79.
2. Malladi, R., J. Sethian, and B. Vemuri, *Shape modeling with front propagation: A level set approach*. IEEE TPAMI, 1995. **17**(2): p. 158-175.
3. Chan, T. and L. Vese, *Active contours without edges*. IEEE Transactions on image processing, 2001. **10**(2): p. 266-277.
4. Leventon, M., W. Grimson, and O. Faugeras. *Statistical shape influence in geodesic active contours*. IEEE CVPR, 2000. p. 316-322.
5. Li, C., C. Xu, C. Gui, and M. D. Fox. *Level set evolution without re-initialization: A new variational formulation*. IEEE CVPR, 2005. Volume 1, p. 430-436.